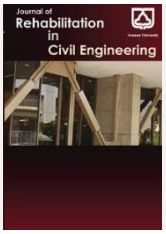

Journal of Rehabilitation in Civil Engineering

Journal homepage: https://civiljournal.semnan.ac.ir/

Effect of Temperature Variation on Rigid Pavement Dowel

Anno Mahfuda [1*]; Suprapto Siswosukarto [2]; Muh Bahrul Ulum Al Karimi [1]

1. Lecturer, Department of Civil Engineering and Planning, Vocational College, Universitas Diponegoro, Jl. Prof. Soedarto No.13, Tembalang, Semarang, Jawa Tengah 50275, Indonesia
2. Lecturer, Department of Civil and Environmental Engineering, Engineering Faculty, Universitas Gadjah Mada, Jl. Grafika No. 2 Yogyakarta, Indonesia

* Corresponding author: annomahfuda@lecturer.undip.ac.id

ARTICLE INFO

Article history:
Received: 31 October 2024
Revised: 21 January 2025
Accepted: 09 March 2025

Keywords:
Rigid pavement;
Dowel;
Thermal gradient;
Finite element method.

ABSTRACT

Given its location along the equator, Indonesia has a tropical climate with two rainy and dry seasons. The significant variations in temperature that each season brings about are important factors when building civil engineering projects, including rigid pavements, to ensure their long-term performance and durability. Currently, rigid pavement design regulations exclude considering the influence of temperature variations. The dowels enormously affect how the rigid pavement system works overall, and joints typically represent the weakest sections in the structure. This study investigates the effects of temperature variations on the stress-strain characteristics of rigid pavements, focusing mainly on dowel behavior. The investigation was conducted through simulation modeling in Abaqus software, incorporating solid 3D elements—specifically hexahedral and tetrahedral types—with materials modeled as homogeneous, isotropic, and linear-elastic. The results indicate that heat conduction in rigid concrete slabs follows a linear pattern, generating tensile stress on the dowels (Sxx=1.719 MPa) and maximum shear stress (Sxy=1.754 MPa), both of which remain below the material's yield stress. The displacement of the dowels varies depending on whether the dowels are fixed or free. Fixed dowels move with the concrete slabs, resulting in lower displacement than free dowels. Thermal loads applied to the upper surface of the rigid pavement led to increased stress and displacement as the temperature rises.

E-ISSN: 2345-4423

How to cite this article:
Mahfuda, A., Siswosukarto, S. and Karimi, M. Bahrul Ulum Al (2026). Effect of Temperature Variation on Rigid Pavement Dowel. Journal of Rehabilitation in Civil Engineering, 14(1), 2200 https://doi.org/10.22075/jrce.2025.35776.2200

1. Introduction

Indonesia experiences a tropical climate due to its location along the equator. As a result, the country only has two seasons: the rainy season and the dry season. During the dry season, regions of Indonesia experience relatively high temperatures and lower humidity, in contrast to the wetter and more humid conditions of the rainy season. Additionally, there are significant variations in daytime and nighttime temperatures across both seasons. These climatic variations are essential considerations in the design of civil engineering structures, such as rigid pavements, to ensure long-term durability. The current design standards for rigid pavements have not to consider the impact of temperature fluctuations and variations on pavement deformation [1]. In rigid pavement construction, the joints represent the weakest points of the structure. Dowels play a crucial role in distributing forces and significantly affect the behavior of rigid pavement structural systems [2]. This study aims to investigate the significant impact of temperature changes and variations on the stress-strain characteristics of rigid pavements, especially on the dowel behavior, using simulation modeling.

The study of temperature effects on rigid pavement in Indonesia has gained attraction, as evidenced by numerous publications on the subject [1–4]. One study indicates that significant stresses and displacements occur in rigid pavement concrete slabs due to temperature gradients caused by conduction and convection from the surrounding environment [1]. For instance, a concrete pavement panel measuring 2.75 x 5 meters may experience stresses of up to 2 MPa due to a temperature difference of 40°C. Another study, utilizing the KENPAVE program and considering various temperature and soil quality factors, analyzed the mechanical behavior of rigid pavement, focusing on stress and deflection. The results suggest that higher temperatures and increased base soil modulus result in more significant stress within rigid pavement structures [2].

Study was also conducted to determine the stress distribution around dowel bars resulting from varying heat gradients in Poland. This study explored the relationship between thermal stress and different dowel bar sizes. It was found that using dowels with smaller diameters leads to increased stress around them. Furthermore, the analysis revealed that a significant amount of tensile stress can be concentrated in the concrete slab on either side of the smaller diameter dowel [5]. Another study investigated the influence of solar radiation (SR) absorption on temperature and thermal stress in Jointed Plain Concrete Pavement (JPCP). A one-dimensional heat transport Model was proposed to predict the temperature distribution along the slab's depth, incorporating both probabilistic and deterministic properties of solar radiation as inputs [3]. Additionally, a finite element method using a three-dimensional approach with Abaqus was employed. The analysis used in Abaqus for the rigid pavement model is Standard Analysis. Abaqus/Standard, the implicit solver, can solve for static equilibrium: the state where the sum of the forces is zero [6]. The results revealed that thermal stress at the corners of the slab significantly impacts critical slab stress more than at other locations. The study also compared the conditions of rigid pavement slabs before and after undergoing polymer grouting repairs. The findings indicated a substantial reduction in critical tensile stress at the corners of the slab due to vehicle and thermal loads. Furthermore, the analysis demonstrated that the stability of the new polymer repair remained effective after three years [4].

Numerical analysis using the Finite Element Method (FEM) provides a more accurate determination of stress and displacement. Spring coefficients are another tool that can enhance the efficiency of the FEM software-based numerical analysis process [7]. By employing elastic elements to connect the two concrete slabs, dowels can also be simulated using beam elements [8]. Utilizing three-dimensional solid parts for modeling allows for the investigation of additional behaviors, such as load distribution friction coefficients, and the visualization of numerical analysis results [9]. This study evaluates the dowels' stress

and displacement resulting from the temperature gradient on top surface of rigid pavement. The Finite Element Method will be applied using three-dimensional elements.

2. Thermal gradient

The processes of convection and heat stress analysis in rigid pavement are interrelated. Convection occurs when there is heat flux on an uninterrupted surface. Heat flux refers to the rate at which heat flows over that surface, measured in watts or joules per second. The measurement of heat flux, expressed in watts per square meter, is obtained by evaluating the temperature gradient across a material with a known thermal conductivity value [10].

Due to temperature differences, convective heat transfer occurs between the flowing air stream and the top surface of the concrete slab [10]. The fluid layer above the slab exhibits varying degrees of coldness and heat, influenced by the surface temperature (Ts) and the ambient air temperature (Ta). The Equation 1 represents the heat convection analysis for the pavement surface.

$$q_c = h_c(T_s - T_a) \quad (1)$$

Where T_a is the temperature of the environment (°C), T_s is the surface temperature (°C), h_c is the convection coefficient ($Wm^{-2}°C^{-1}$), and q_c is the convective heat flux (Wm^{-2}). An empirical approach has been proposed to determine the coefficient of convective heat transfer, as well as to account for wind speed and the roughness of the continental surface [10].

3. Research method

A rigid pavement construction in a specific area of DIY was chosen to represent rigid pavement across the different districts in the region. Using the geometric characteristics of the road, a model was created to simulate how the rigid pavement behaves in response to temperature variations.

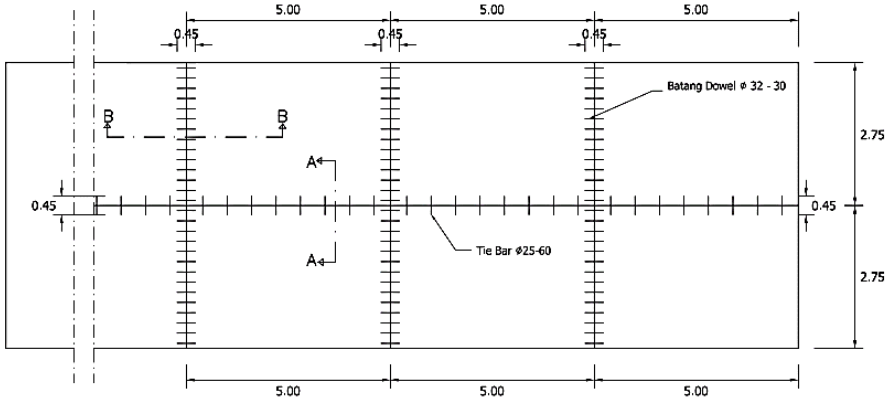

Fig. 1. The geometry of the rigid pavement section.

The developed model consists of six concrete slab panels with thickness of 25 cm joined by dowels and tie bars, as shown in Figure 1. A 10 cm thickness layer of lean concrete used as the subbase for the rigid pavement, supported by subgrade material with a CBR value of 6% with 300 cm thickness. The dowels were modeled closely to match real conditions, with a diameter of 32 mm, a length of 46 cm, and a minimum bend of BJ 370. This configuration adheres to the design guidelines set by the Sleman District Transportation Regulation in Yogyakarta, Indonesia.

This study considered several temperature variations: 50°C, 45°C, and 40°C during the day, and 25°C, 28°C, and 30°C at night. These temperatures were recorded in Sleman, Yogyakarta, in August and

September 2024, at the surface of a rigid pavement concrete slab. A calibrated thermometer was used for these measurements and the results are shown in Figure 2. The linear variation in temperatures was also analyzed, suggesting that the concrete slab's top and bottom surfaces can exhibit different temperature gradients. To determine the temperature differential within the concrete slab, a numerical approach was applied [11,12]. The results show a positive gradient of 0.66°C/cm and a negative gradient of -0.33°C/cm.

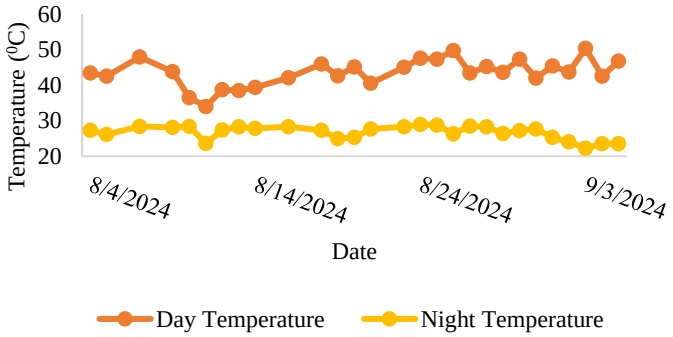

Fig. 1. Temperature measurement between August-September 2024 at Sleman, Yogyakarta.

The structural model of the rigid pavement was modelled using Abaqus simulation. Hexahedral and tetrahedral 3D solid elements were used in the modeling process. The system was refined to integrate the thermal properties and parameters of the rigid pavement. These include each material or layer's thermal conductivity, coefficient of expansion, and specific heat, as detailed in Table 1. the majority of the materials in the subgrade, sub-base, and base layers are non-plastic (NP), according to the results of the test of Atterberg limits determination of the pavement layers [13]. The model also assumes isotropic, homogeneous, and linear-elastic materials [14]. To ensure accuracy, the modeling began with a convergence test, using 20 cm mesh sections, meaning the rigid pavement was divided into 20 cm by 20 cm segments [14]. Figure 4a shows the global mesh used in the pavement modeling, while Figure 4b illustrates the mesh between layers and elements. The specific dowel element is depicted in Figure 4c.

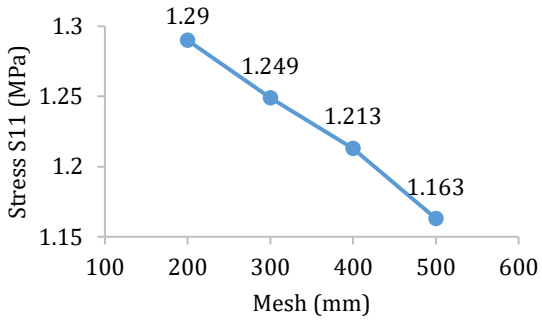

Fig. 2. Convergence test on rigid pavement model.

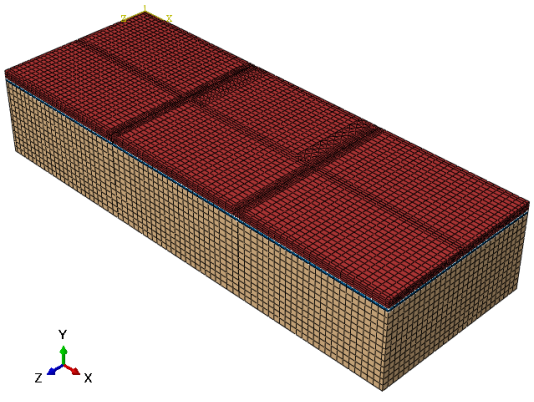

(a)

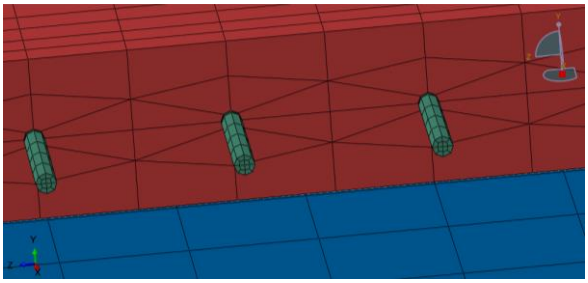

(b)

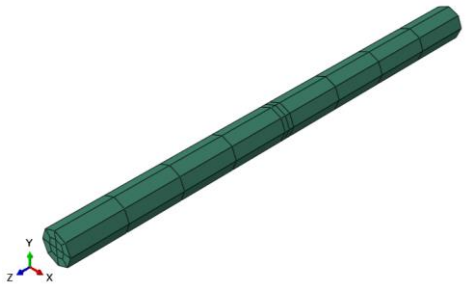

(c)

Fig. 3. Global mesh in rigid pavement modelling (a); Mesh between slab, dowel, sub-base, and subgrade (b); Dowel mesh in rigid pavement modelling (c).

Table 1. Property of materials in rigid pavement model [1].

Materials	Parameters	Value	Unit	Reference
Concrete	Compressive Strength (f'c)	41.33	MPa	[15]
	Elasticity Modulus	30215.55	MPa	[16]
	Poisson Ratio	0.25		[17]
	Density	2.4x10-9	Ton mm^{-3}	[17]
	Conductivity (k	1.4	mW $mm^{-1}°C^{-1}$	[18]
	Specific Heat (Cp)	8.8x108	mJ $ton^{-1}°C^{-1}$	[18]
	Coefficient of Thermal Expansion (α)	1.2x10-5	°C	[18]
Dowel	Elasticity Modulus	200000	MPa	[17]
	Poisson Ratio	0.3		[17]
	Density	7.85	Ton mm^{-3}	[17]
	Conductivity (k)	45.3	mW $mm^{-1}°C^{-1}$	[18]
	Specific Heat (Cp)	5.02x108	mJ $ton^{-1}°C^{-1}$	[18]
Lean Concrete	Compressive Strength (f'c)	10	MPa	[15]
	Elasticity Modulus	14862.71	MPa	[16]
	Poisson Ratio	0.25		[17]
	Density	2.4x10-9	Ton mm^{-3}	[17]
	Conductivity (k)	1.4	mW $mm^{-1}°C^{-1}$	[18]
	Specific Heat (Cp)	8.8x108	mJ $ton^{-1}°C^{-1}$	[18]
Subgrade	CBR	6	%	
	Elasticity Modulus	0.04	MPa	[19]
	Poisson Ratio	0.3		[20]
	Density	1.78x10-9	Ton mm^{-3}	[21]
	Conductivity (k	1.675	mW $mm^{-1}°C^{-1}$	[18]
	Specific Heat (Cp)	1.381x10-9	mJ $ton^{-1}°C^{-1}$	[18]

The dimensions and material properties of the elements were included in the model from the collected data. Assumptions from previous studies were applied to model interactions between the rigid pavement layers. The following assumptions were used [1,14]: Surface-to-surface contact was applied as the specific interaction type between the layers. The friction coefficient between the dowel fixed by rigid

pavement panel is 0,9 according to earlier study [22]. The friction coefficient between the dowel that free to slide (sliding side) by rigid pavement panel is 0,1 according to previous research [22]. The rigid pavement panels are on top of subbase or lean concrete with a Polyethylene layer with an implemented friction coefficient by 0,252 [23]. The subgrade layer in this model has 0,4 of friction coefficient with the subbase layer that placed on top of the surface [24]. The couple-temperature displacement was employed as the analysis step in the modeling process. The temperature load was applied only to the rigid pavement concrete slab, with temperature values based on the thermal gradient at both the top and bottom of the slab. Under the boundary conditions, the structure can deform vertically except for the underlying soil, which remains fixed. Due to their infinite domain and symmetry, all subgrade planes are restricted from horizontal deformation. Similarly, the two concrete slabs are also constrained from horizontal bending, except along the plane of symmetry [14].

4. Results

The effects of temperature variations were analyzed through rigid pavement modeling using Abaqus, focusing on the stress-strain behavior around the dowel bars. Figures 8 and 9 illustrate how stress develops in the dowels as temperatures increase on the concrete slab's surface. The conduction process is expected to generate linear changes in the heat transfer process in rigid pavement concrete slabs. Conduction process into the rigid concrete slab's body through the slab's surface, which is assumed to receive heat through convection. The temperature of the concrete slab will increase linearly by 0.33 ^{0}C/cm when the temperature is 25 ^{0}C or at night (negative gradient) [11,12]. The temperature of the concrete slab will increase linearly by 8.25 ^{0}C, equivalent to 33.25 ^{0}C, at a thickness of 25 cm as shown in Figure 5a. The temperature on the concrete slab will decrease by 0.66 C/cm since the surface of the upper concrete slab has a temperature of 50 ^{0}C. The temperature of the concrete slab is 43.4 ^{0}C at a thickness of 10 cm. The temperature of the concrete slab will be 33.5 ^{0}C at a thickness of 25 cm. Figure 5b shows the transfer process at the concrete slab's surface temperature of 50 ^{0}C or during the day (positive gradient).

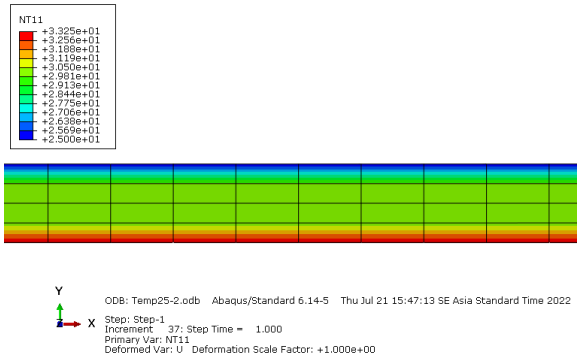

(a)

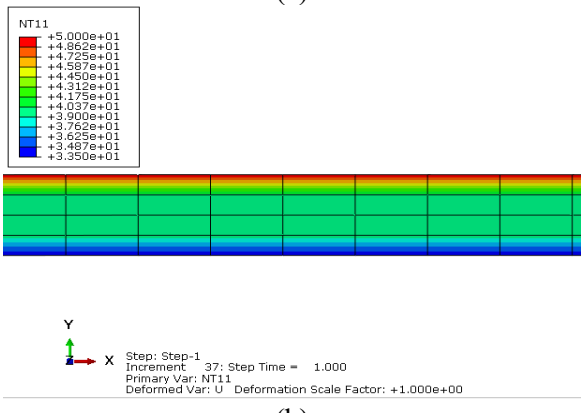

(b)

Fig. 5. Heat transfer in rigid pavement model due to temperature load at 25°C (a); Heat transfer in rigid pavement model due to temperature load at 50°C (b).

Various displacements and stress distributions will occur in the concrete slab due to temperature variations, influenced by positive and negative gradients resulting from the conduction process. During the day, the upper surface of the concrete slab will have significant tensile stress, while the lower surface will be under compressive stress. The highest stress level will occur at the center of the slab's surface. Figure 12 illustrates this effect when a 50°C temperature is applied to the slab's upper surface. In contrast, at 25°C, the upper surface of the concrete slab will undergo compressive stress, while the lower surface will have tensile stress. Figure 7 shows this effect at 25°C on the upper surface of the concrete slab. Since the dowel element plays a critical role in distributing the stress across the slab panels, allowing the concrete slab to function as an integrated structure, the results of these two analyses will directly influence the performance of the dowels. The numerical analysis result demonstrates the stress temperature effect similar pattern to that result in previous studies [4,25–27].

The concrete slab have the stress due to temperature variations on its upper surface in a rigid pavement. This will influence the dowel elements placed within the rigid pavement concrete slab. The highest values for tensile normal and shear stress will be used in this study as the stress values. The dowel part receives significant displacement and produces the stress value used in this study. In this study, the authors uses a dowel in the center of a rigid pavement panel as an illustration. As shown in Figure 7, the stress distribution on the center concrete slab surface has a relatively high value.

At a surface temperature of 50°C, the concrete slab have a maximum tensile dowel stress of 1.719 MPa at Sxx. This stress is still below the dowel's yield stress of 240 MPa. In contrast, at a surface temperature of 25°C, the tensile dowel stress is at its lowest, measuring 0.01934 MPa at Szz, which is also well below the dowel's yield stress. The analysis shows a clear pattern: stress increases as the concrete slab's surface temperature rises. This trend is illustrated in Figure 6a and is consistent with previous findings reported in previous finding [4,25–27].

At a surface temperature of 50°C, the concrete slab generates a maximum shear dowel stress of 1.754 MPa at Sxy, which is still below the dowel's yield stress of 240 MPa. Conversely, at a surface temperature of 25°C, the shear dowel stress is at its lowest, measuring 0.0183 MPa at Sxz, which remains well below the dowel's yield stress. The analysis reveals a clear pattern: shear stress increases as the surface temperature of the concrete slab rises. This trend is illustrated in Figure 6b.

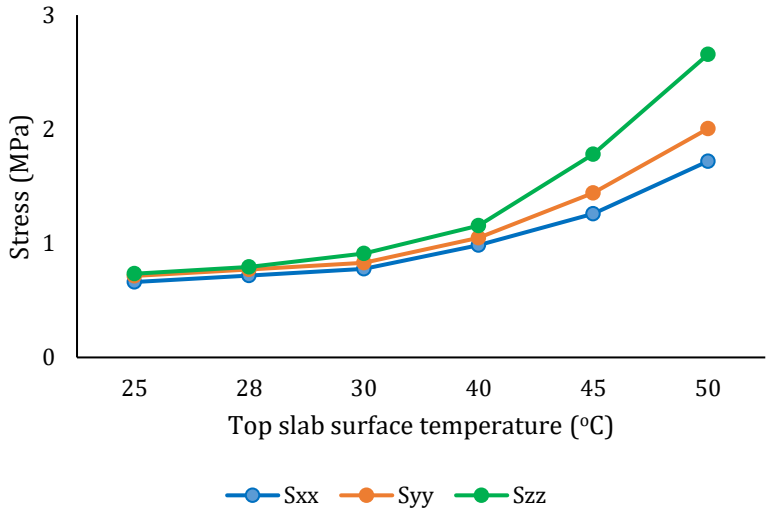

(a)

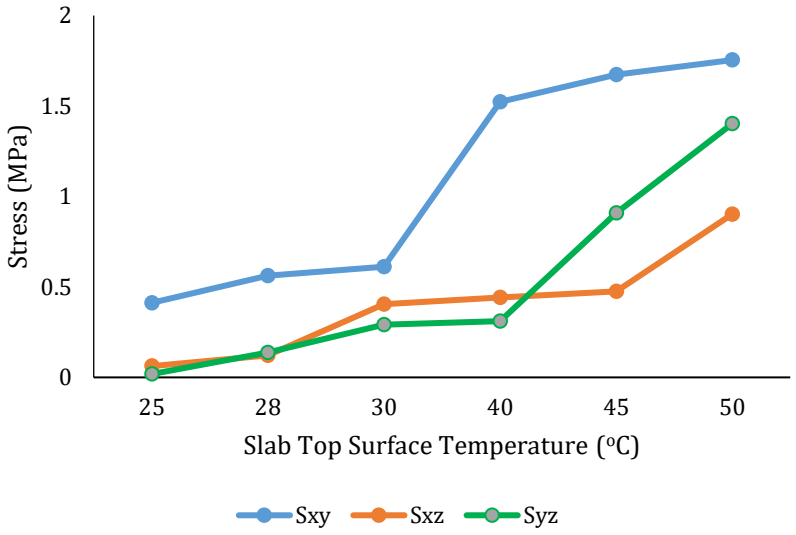

(b)

Fig. 6. Tensile normal stress on the influence of temperature on the rigid pavement dowel (a); Tensile shear stress on the influence of temperature on the rigid pavement dowel (b).

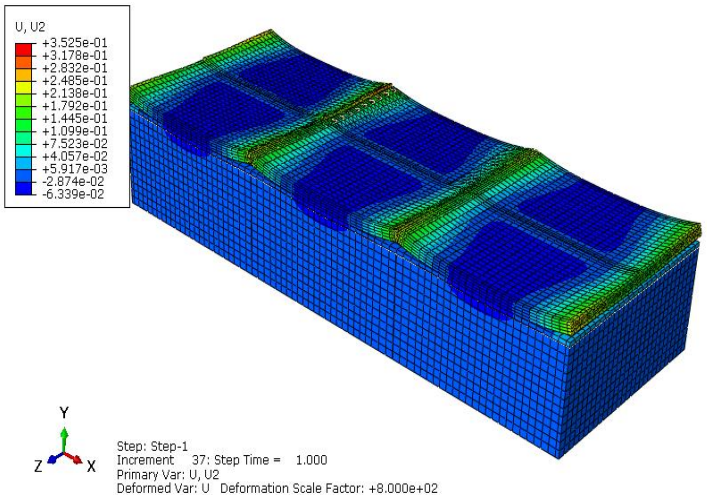

(a)

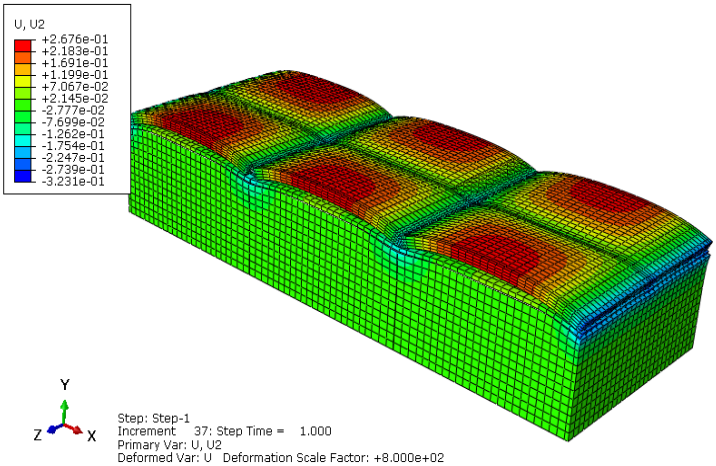

(b)

Fig. 7. Displacement (U2) contour in Rigid Pavement due to temperature load at 25°C (deform sale: 800) (a); Displacement (U2) contour in Rigid Pavement due to temperature load at 50°C (deform sale: 800) (b).

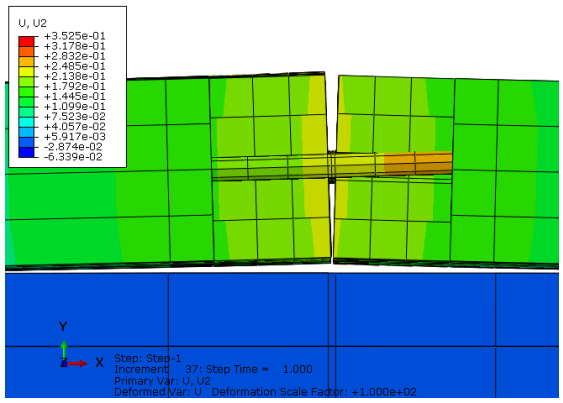

(a)

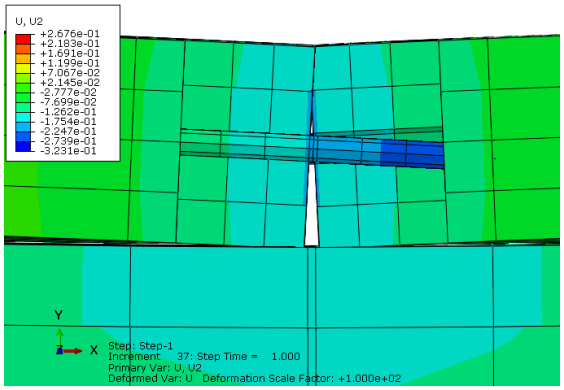

(b)

Fig. 8. Displacement (U2) contour in dowel due to temperature load at 25°C (deform scale: 100) (a); Displacement (U2) contour in dowel due to temperature load at 50°C (deform scale: 100) (b).

Displacement in the dowel section results from temperature variations affecting the rigid pavement concrete slab. These temperature-induced changes cause the dowel to deform in multiple directions, such as U1, U2, and U3, as shown in Figure 7. For instance, Figure 8 illustrates that the dowel bends toward the Y-axis (U2). The assessment of maximum and minimum displacements is based on measurements between the dowels. When the surface temperature of the concrete slab reaches 25°C, the dowel experiences the maximum tensile displacement at U2, with a value of 0.977 mm, as shown in Figure 11a. The minimum tensile displacement occurs at U3, measuring 0.0255 mm. In contrast, the maximum compressive displacement occurs at U2, with a value of 0.413 mm, and the minimum compressive displacement is observed at U1, with a value of -0.1897 mm, as shown in Figure 11b. As the surface temperature of the concrete slab increases, the displacement values change significantly. When the surface temperature reaches 50°C, the dowel experiences a maximum tensile displacement at U2, with a value of 0.0563 mm, as shown in Figure 11a. The minimum tensile displacement at U3 is 0.00148 mm. Conversely, the maximum compressive displacement occurs at U1, with a value of 0.0316 mm, and the minimum compressive displacement is observed at U2, with a value of -0.117 mm, as shown in Figure 11b.

Displacement within the dowel element in this research has particular characteristics. Results show reactions of displacement that are typically in line with the results in earlier study. This is because the restraining and free principles are utilized in the dowel used in this research. The fixed dowel is the side immediately embedded in the concrete without any interference or continuous material that creates a connection between the dowel surface and the concrete surface with a specific coefficient of friction. The

free side of the dowel refers to the side that has been embedded, but a medium separates the concrete surface and the dowel surface.

When the top surface of the concrete slab reaches a temperature of 25°C, it will have displacement. Figure 8a shows the difference in displacement contours at U2 for fixed and free dowels. The fixed dowel showed tensile displacement, causing a tensile displacement of 0.0213 mm. This effect from the fixed dowel deforms from the top surface of the concrete slab down to the bottom. In contrast, the free dowel section only shows tensile displacement effects within a radius of 20 cm around the dowel with 0,349 mm. This is due to the free dowel were having higher tensile stress than the fixed dowel. A comparison of the dowel's displacement values can be seen in Figure 10, which analyzes a specific path or line defined at the dowel located in the middle of the wide side of the concrete slab, as depicted in Figure 9.

Conversely, when the top surface of the concrete slab reaches a temperature of 50°C, it will also experience displacement. Figure 8b illustrates the differences in displacement contours at U2 for fixed and free dowels. The fixed dowel exhibits tensile displacement, causing a compressive displacement of -0.0754 mm. This effect from the fixed dowel deforms from the top surface of the concrete slab down to the bottom. Similarly, in the free dowel section, the compressive displacement effect, with -0,268 mm, also extends from the top surface of the concrete slab around the dowel to the bottom. A comparison of the displacement values of the dowel can be seen in Figure 10, which analyzes a specific path or line defined at the dowel located in the middle of the wide side of the concrete slab, as depicted in Figure 9.

According to [28], c

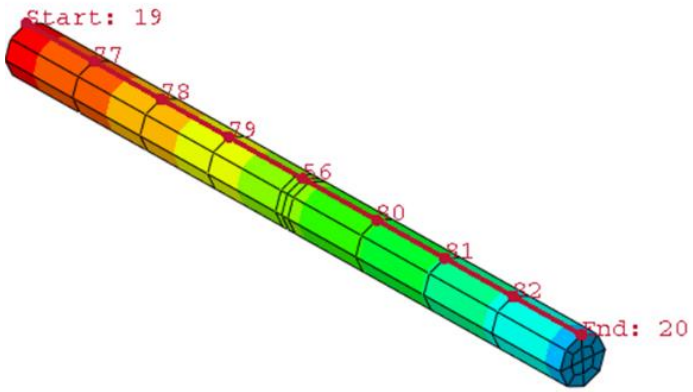

Fig. 9. Path on dowel in rigid pavement model.

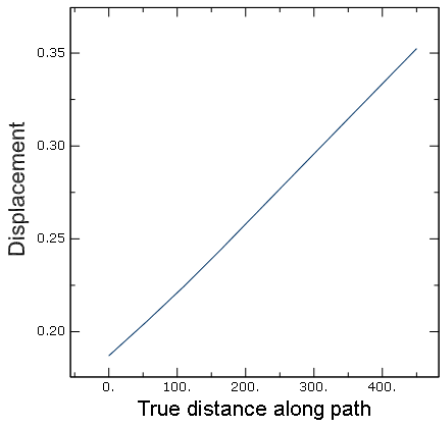

(a)

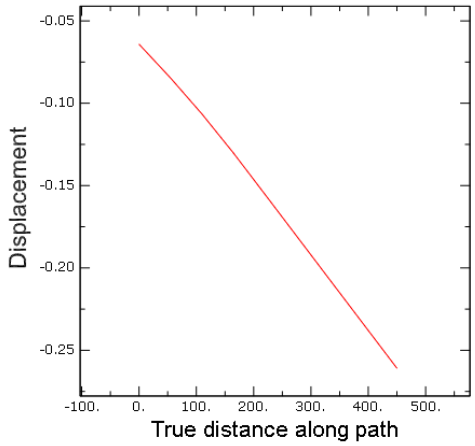

(b)

Fig. 10. The displacement of the dowel due to temperature influence on slab top surface (a) temperature 25°C, (b) temperature 50°C.

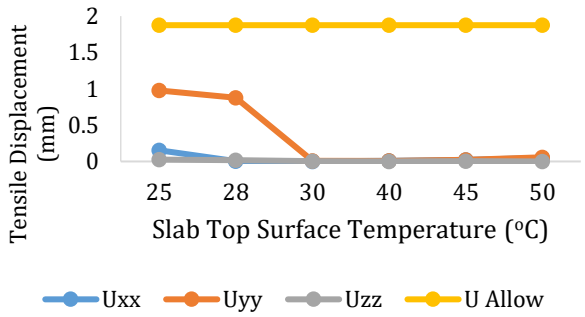

(a)

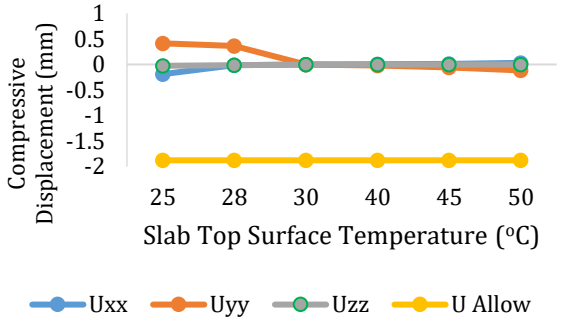

(b)

Fig. 4. Tensile displacement on the dowel due to temperature influence on slab top surface (a); Compressive displacement on the dowel due to temperature influence on slab top surface (b).

According to the results of the finite element analysis, the concrete slab that attaches the dowel will eventually come into contact with the deflection and stress that occur. Because thermal stress is closely related to the stress and deflection of the concrete slab, it is important to reduce or minimize the size of the rigid pavement panel. As a result, it is necessary to assess the size of the existing concrete plate so that the dimensions used ideally comply with the applicable AASHTO standards. [29]. Rehabilitation needs to be performed to compensate for the temperature load that has occurred in order to prevent damage to the concrete slab from the stress and deflection that the dowel has received. According to Dita's research [30], one technique that can be applied in the repair process is applying bacteria to concrete pavement. The rehabilitation of rigid pavement may also be undertaken by adding asphalt toppings to reduce the

thermal load that the surface will take [31]. Previous studies have shown that an asphalt-based method is also suitable for restoring damage to concrete slabs [32]. Concrete slab panels may be made by modifying the section of the slab which comes through contact with the dowel, in accordance to previous finding [33]. This provides for the anticipating of deflection on the dowel before it comes into direct contact with the concrete.

Conclusion

The results of the study showed that heat conduction in rigid concrete slabs occurs linearly at temperatures of 25°C and 50°C on their upper surface, influencing the dowel stress. At 50°C, the highest normal tensile stress at Sxx is 1.719 MPa, which is less than the yield stress. Similarly, at the same temperature, the greatest shear stress at Sxy is 1.754 MPa, which is likewise lower than the yield stress. The displacement caused by the stress placed on the dowels is as follows: at 50°C, the maximum tensile displacement is 0.0563 mm at U2, and at 25°C, it is 0.977 mm at U2. Furthermore, there are conduct variations between fixed and free dowels. Fixed dowels tend to move with the concrete slabs, causing lower displacements than free dowels. Tensile displacement at U2 at 25°C is 0.0213 mm for fixed dowels and 0.349 mm for free dowels. The confined dowel's compressive displacement at 50°C is -0.0754 mm at U2, while the free dowel has a compressive displacement of -0.268 mm.

Author Contribution Statement

Anno Mahfuda: Roles/Writing – original draft, Software, and Conceptualization.

Suprapto Siswosukarto: Conceptualization, Software, Supervision, Validation, and Methodology.

Muh Bahrul Ulum Al Karimi: Roles/Writing – original draft and Writing – review & editing.

References

[1] Mahfuda A, Siswosukarto S, Suhendro B. The Influence of Temperature Variations on Rigid Pavement Concrete Slabs. J Civ Eng Forum 2023;9:139–50. https://doi.org/10.22146/jcef.5744.

[2] Setiawan DM. The role of temperature differential and subgrade quality on stress, curling, and deflection behavior of rigid pavement. J Mech Behav Mater 2020;29:94–105. https://doi.org/10.1515/jmbm-2020-0010.

[3] Cui C, Lu Q, Guo C, Wang F. Analysis of the Coupling Effect of Thermal and Traffic Loads on Cement Concrete Pavement with Voids Repaired with Polymer Grout. Adv Mater Sci Eng 2022;2022. https://doi.org/10.1155/2022/2517250.

[4] MacKiewicz P. Thermal stress analysis of jointed plane in concrete pavements. Appl Therm Eng 2014;73:1169–76. https://doi.org/10.1016/j.applthermaleng.2014.09.006.

[5] Kim J, Hjelmstad KD. Three-Dimensional Finite Element Analysis of Doweled Joints for Airport Pavements. Transp Res Rec 2003:100–9. https://doi.org/10.3141/1853-12.

[6] Abaqus/CAE Guide User. ABAQUS/CAE 6.14 USER'S GUIDE. United States of America: Dassault Systèmes Simulia Corp; 2014.

[7] Qin Y, Hiller JE. Modeling the temperature and stress distributions in rigid pavements: Impact of Solar Radiation absorption and heat history development. KSCE J Civ Eng 2011;15:1361–71. https://doi.org/10.1007/s12205-011-1322-6.

[8] Timoshenko, Woinowski. Theory of Plates and Shells. vol. 67. United States of America: McGraw-Hill Book Company; 1974. https://doi.org/10.1016/0006-8993(74)90278-9.

[9] Kim K, Chun S, Han S, Tia M. Effect of Dowel Bar Arrangements on Performance of Jointed Plain Concrete Pavement (JPCP). Int J Concr Struct Mater 2018;12. https://doi.org/10.1186/s40069-018-0276-1.

[10] Huang K, Zollinger DG, Shi X, Sun P. A developed method of analyzing temperature and moisture profiles in rigid pavement slabs. Constr Build Mater 2017;151:782–8. https://doi.org/10.1016/j.conbuildmat.2017.06.120.

[11] Huang YH. Pavement Analysis and Design, Second Edition. United States of America: Pearson Prentice Hall; 2004.

[12] Khan MI, Qadeer MA, Harwalkar AB. Mechanistic Analysis of Rigid Pavement for Temperature Stresses Using Ansys. IOSR J Mech Civ Eng 2014;11:90–107. https://doi.org/10.9790/1684-112790107.

[13] Farahani HZ, Farahani A. Study on Drainage of Pavement Layers and Improvement Strategies: Case Study. J Rehabil Civ Eng 2023;11:111–26. https://doi.org/10.22075/JRCE.2022.25393.1575.

[14] El-nakib M. Faulting in rigid pavement system of highways 2007;44:581–4.

[15] DPUPKP of Sleman Regency. Dinas Pekerjaan Umum, Perumahan dan Kawasan Permukiman Kabupaten Sleman. Indonesia: 2021.

[16] SNI 2847:2019. Persyaratan Beton Struktural Untuk Bangunan Gedung. 2019.

[17] Tyau JS. Finite Element Modelling Of Reinforced Concrete Using 3- Dimensional Solid Elements With Discrete Rebar. Master Deg, United States of America: Department of Civil and Engineering, Birgham Young University; 2009, p. 1–78.

[18] Prawesti P. ANALISIS BEBAN EKUIVALEN RODA TUNGGAL DUAL-TRIDEM PESAWAT BOEING 777-300ER PADA PERKERASAN KAKU DENGAN METODE ELEMEN HINGGA, Yogyakarta: MSTT UGM; 2018, p. 1–172.

[19] Aulia G. Evaluasi Penggunaan Controlled Modulus Columns (CMC) Di Bandara Soekarno-Hatta, Yogyakarta: FT UGM; 2015, p. 1–110.

[20] Bowless JE. Foundation Analysis and Design. 5th Edition. 5th ed., United States of America: The McGraw-Hill; 1997, p. 1–1247.

[21] Saffar AKK Al, Behaya SAM, Jassim HSH, Ajam HKK. Empirical Equation Correlate California Bearing Ratio (CBR) with Dry Density for Granular Soil. AcademiaEdu 2021;10:300–3.

[22] Keymanesh MMR, Mirshekari Babaki M, Shahriari N, Pirhadi A, Mirshekarian Babaki M, Shahriari N, et al. Evaluating the Performance of Dowel in PCC Pavement of Roads using ABAQUS Finite Element Software. Int J Transp Eng 2018;5:349–65.

[23] Pettersson D, Alemo J. Characterization of restraint from friction tests with slabs cast on ground. Struct Concr 2000;1:181–7. https://doi.org/10.1680/stco.2000.1.4.181.

[24] William GW, Shoukry SN. 3D Finite Element Analysis of Temperature-Induced Stresses in Dowel Jointed Concrete Pavements. Int J Geomech 2001;1:291–307. https://doi.org/10.1061/(asce)1532-3641(2001)1:3(291).

[25] Abu El-Maaty AE, Hekal GM, Salah El-Din EM. Modeling of Dowel Jointed Rigid Airfield Pavement under Thermal Gradients and Dynamic Loads. Civ Eng J 2016;2:38–51. https://doi.org/10.28991/cej-2016-00000011.

[26] Chai G, Staden R van, Guan H, Loo Y-C. Impact of Climate Related Changes in Temperature on Concrete Pavement: A Finite Element Study. 25th ARRB Conf Futur Link Policy, Res Outcomes 2012:1–12.

[27] Zhou B, Pei J, Zhang J, Wang C. Joint design and load transfer capacity analysis of photovoltaic/thermal integrated pavement unit. J Clean Prod 2022;380:135029. https://doi.org/10.1016/j.jclepro.2022.135029.

[28] SNI 1729:2020. Spesifikasi Untuk Bangunan Gedung Baja Struktural. Sni 1729-2020 2020:1–336.

[29] AASHTO. Design of Pavement Structures, 1993.

[30] Ariyanti D, Sasongko NA, Fansuri MH, Fitriana EL, Nugroho RA, Pratiwi SA. Retrofitting of concrete for rigid pavement using bacterial: A meta-analysis. Sci Total Environ 2023;902:166019. https://doi.org/10.1016/j.scitotenv.2023.166019.

[31] Rahmani M, Kim YR. Coupled thermo-mechanical modeling of reflective cracking in flexible pavements. Int J Solids Struct 2025;308:113129. https://doi.org/10.1016/j.ijsolstr.2024.113129.

[32] Dhakal N, Elseifi MA, Zhang Z. Mitigation strategies for reflection cracking in rehabilitated pavements – A synthesis. Int J Pavement Res Technol 2016;9:228–39. https://doi.org/10.1016/j.ijprt.2016.05.001.

[33] Guo J, Chan TM, Wang Y. Precast concrete pavement applications, design and joint load transfer characteristics. Structures 2024;69:107176. https://doi.org/10.1016/j.istruc.2024.107176.